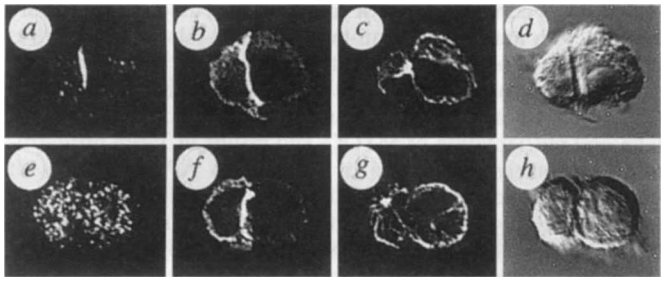

FIG. 5 Only APCs pulsed with high concentrations of antigen that induce full activation of T cells can cause the translocation of PKC-θ. CH12 cells were pulsed with 500 μg ml^{-1} (*a–d*) or 0.5 μg m^{-1} (*e–h*) of conalbumin. D10–CH12 cojugates were triply labelled with anti-PKC-θ (*a*, *e*), talin (*b*, *f*) or tubulin (*c*, *g*). Note that PKC-θ is not clustered at the contact in the cell conjugate in which the MTOC is not facing the contact area.

proliferation of AK8 cells, resulted in the formation of significantly fewer Th–APC conjugates (about 20% of control levels). Talin was still clustered in most (70.5 ± 15%) of these conjugates, indicating some activation, but PKC-θ clustering was only very rarely (2% ± 1%) observed in these conjugates (data not shown).

The lack of PKC-θ translocation in antibody-activated T cells and in APC-activated T-cell hybridomas further supports the idea that PKC-θ participates in the induction of T-cell response to antigen. Treatment of D10 cells with anti-TCR/CD3 monoclonal antibodies induces cytokine production, but the cells later fail to proliferate and they undergo apoptosis (ref. 18, and C.R.F.M. *et al.*, unpublished data). Similarly, the activated T-cell hybridomas produce cytokines but fail to proliferate, and later undergo apoptosis[19,20]. Taken together, these suggest that PKC-θ is involved in TCR-dependent proliferation, but not in triggering cytokine production. In summary, our studies at the single-cell level identified PKC-θ as being selectively affected during the interaction of T cells with their APC. Further studies are needed to identify the role and molecular basis for the unique response of this enzyme. □

Methods

Immunofluorescence microscopy. The cloned Th cell line D10.G4.1 (D10) is specific for the egg-white protein conalbumin and for IAK, and was used previously[13]. D10-IL2 is a subclone of D10. The B-cell lymphoma CH12.LX (CH12) (IAK) was used as an APC. D10 cells were mixed at a 1:1 cell ratio with CH12 cells that were pulsed overnight with conalbumin (500 μg ml^{-1}). Cell conjugates were formed and processed[5]. The affinity-purified rabbit antibodies against the PKC isoforms (Santa Cruz) were directed against unique peptide sequences at the C-terminal region of the proteins. Western blots with the anti-PKC-θ antibody labelled a single band (M_r ~80K) in GP&E fibroblasts that were infected with a retroviral vector encoding for PKC-θ, and did not detect any protein bands in the parental uninfected cells (data not shown). The ability of each of these antibodies to detect the specific PKC isoforms by immunofluorescence microscopy was confirmed by labelling, either in the presence or absence of TPA, a panel of fibroblast cell lines that overexpressed each of the PKC isoforms (data not shown). The immunofluorescence and the corresponding Normarski images of the cells were recorded by a chilled charge-coupled device digital camera (MCD1000, Spectra Source) that was mounted on a Zeiss Axiophot microscope, equipped with narrow-band optical filters (Chromatech). Images were processed by a no-neighbour deconvolution program to remove out-of-focus haze[5]. At least 400 cells were analysed per coverslip.

***In vitro* kinase assays.** Conjugates of D10 (4×10^6 cells per assay) and CH12 (2×10^6 cells per assay) were formed as before, and 20 min later the cells were washed once in PBS and lysed (100 μl of 20 mM Tris, pH 7.6, and 0.5% NP-40, 0.25 M NaCl, 3 mM EDTA, 3 mM EGTA, 1 mM PMSF, 2 mM Na_3VO_4, 20 μg m^{-1} Aprotinin, 100 μg ml^{-1} Leupeptin, 1 mM DTT). After centrifugation, PKC-θ and PKC-δ were immunoprecipitated with the affinity-purified rabbit antibodies (1 μg) coupled to protein A Sepharose beads. The beads were washed in PKC-kinase buffer (20 mM HEPES, pH 7.2, and 137 mM NaCl, 5.4 mM KCl, 0.3 mM NaH_2PO_4, 0.4 mM KH_2PO_4, 25 mM β-glycerophosphate, 10 mM $MgCl_2$, 5 mM EGTA and 2.5 mM $CaCl_2$). The kinase assay was performed by adding 35 μl of kinase buffer containing 0.1 mM ATP, [γ-^{32}P]ATP (20 μCi per assay) and 0.1 mM Selectide PKC substrate (CalBiochem) for 20 min at 30 °C. The reactions were stopped by the addition of 10 μl 25% TCA. The reaction mixtures were blotted on P81 phosphocellulose paper, washed with 75 mM phosphoric acid to remove free ATP, dehydrated and counted in a scintillation counter (Beckman). For each set of conditions, reactions were also performed in the absence of the Selectide substrate. The level of phosphorylation of the substrate was determined by subtracting the radioactive counts that were obtained in the absence of the substrate from those obtained in its presence. In each case a parallel reaction mixture contained also 125 ng ml^{-1} TPA, which causes maximal activation of the PKC that is present in the immunoprecipitate. Duplicate samples were analysed for each assay.

Received 9 August; accepted 8 November 1996.

1. Hug, H. & Sarre, T. F. *Biochem. J.* **291,** 329–343 (1993).
2. Baier, G. *et al. Eur. J. Biochem.* **225,** 195–203 (1994).
3. Weiss, A. & Littman, D. R. *Cell* **76,** 263–274 (1994).
4. Podack, E. R. & Kupfer, A. *Annu. Rev. Cell Biol.* **7,** 479–504 (1991).
5. Kupfer, H., Monks, C. R. & Kupfer, A. *J. Exp. Med.* **179,** 1507–1515 (1994).
6. Osada, S. *et al. Mol. Cell. Biol.* **12,** 3930–3938 (1992).
7. Baier, G. *et al. J. Biol. Chem.* **268,** 4997–5004 (1993).
8. Yamada, K. *et al. Biochem. J.* **308,** 177–180 (1995).
9. Kupfer, A. & Singer, S. J. *J. Exp. Med.* **170,** 1697–1713 (1989).
10. Chen, S. J. *et al. Biochemistry* **32,** 1032–1039 (1993).
11. Robles-Flores, M. & Garcia-Sainz, J. A. *Biochem. J.* **296,** 467–472 (1993).
12. Mochly-Rosen, D. *Science* **268,** 247–251 (1995).
13. Kupfer, A. *et al. Proc. Natl Acad. Sci. USA* **84,** 5888–5792 (1987).
14. Kupfer, A. & Singer, S. J. *Annu. Rev. Immunol.* **7,** 309–337 (1989).
15. Kupfer, A., Burn, P. & Singer, S. J. *J. Mol. Cell. Immunol.* **4,** 317–325 (1990).
16. Rojo, J. M., Kerner, J. D. & Janeway, C. Jr *Eur. J. Immunol.* **19,** 2061–2067 (1989).
17. Yoon, S. T., Dianzani, U., Bottomly, K. & Janeway, C. A. Jr *Immunity* **1,** 563–569 (1994).
18. Cherwinski, H. M., Semenuk, G. T. & Ransom, J. T. *J. Immunol.* **148,** 2996–3003 (1992).
19. Harwell, L., Skidmore, B., Marrack, P. & Kappler, J. *J. Exp. Med.* **152,** 893–904 (1980).
20. Yang, Y., Mercep, M., Ware, C. F. & Ashwell, J. D. *J. Exp. Med.* **181,** 1673–1682 (1995).

ACKNOWLEDGEMENTS. These studies were supported in part by grant from the NIH.

CORRESPONDENCE and requests for materials should be addressed to A.K. (e-mail: kupfera@njc.org).

RAIDD is a new 'death' adaptor molecule

Hangjun Duan & Vishva M. Dixit

Department of Pathology, University of Michigan Medical School, Ann Arbor, Michigan 48109, USA

THE effector arm of the cell-death pathway is composed of cysteine proteases belonging to the ICE/CED-3 family[1,2]. In metazoan cells these exist as inactive polypeptide precursors (zymogens), each composed of a prodomain, which is cleaved to activate the protease, and a large and small catalytic subunit. The coupling of these 'death' proteases to signalling pathways is probably mediated by adaptor molecules that contain protein–protein interaction motifs such as the death domain[1]. Here we describe such an adaptor molecule, RAIDD, which has an unusual bipartite architecture comprising a carboxy-terminal death domain that binds to the homologous domain in RIP, a serine/threonine kinase component of the death pathway[3,4]. The amino-terminal domain is surprisingly homologous with the sequence of the prodomain of two ICE/CED-3 family members, human ICH-1 (ref. 5) and *Caenorhabditis elegans* CED-3 (ref. 6). This similar region mediates the binding of RAIDD to ICH-1 and CED-3, serving as a direct link to the death proteases, indicating that the prodomain may, through homophilic interactions, determine the specificity of binding of ICE/CED-3 zymogens to regulatory adaptor molecules. Finally, alternations in the sequence of the N-terminal domain that are equivalent to inactivating mutations in the *C. elegans ced*-3 gene[7,8] prevent homophilic binding, highlighting the potentially primordial nature of this interaction.

A sequence (IMAGE Consortium CloneID 109053) was identified in the NCBI GenBank expressed-sequence tag (EST) data base as having statistically significant homology ($P < 0.001$) to the prodomain of the human ICE-like protease ICH-1. This EST clone was used to isolate a full-length complementary DNA that encoded a protein of 200 amino acids with a predicted relative molecular mass of 22K (Fig. 1*a*). Given its sequence and interac-

tions (see below), this molecule was designated RAIDD (for RIP-associated ICH-1/CED-3-homologous protein with a death domain) (Fig. 1). A BLAST search revealed that this was a new molecule with two domains that had distinct homologies: residues 8–80 had statistically significant homology ($P < 0.001$) with the prodomains of the human ICE-like protease ICH-1 and the *C. elegans* death protease CED-3 (Fig. 1*b*). Residues 123–195 encoded a death domain with significant homology to other death-domain-containing adaptor molecules (Fig. 1*c*). Northern blot analysis revealed RAIDD to be constitutively expressed as a 1.35-kilobase (kb) transcript in all adult and fetal tissues examined, with particularly high expression in adult heart, testis, liver, skeletal muscle, fetal liver and kidney (Fig. 1*d*).

The homology between the N-terminal domain (NTD) of RAIDD and the prodomains of ICH-1 and CED-3 suggested that RAIDD probably binds ICH-1 and CED-3 through a homophilic mechanism using this homologous interaction domain. We investigated this possibility by examining the interaction of ^{35}S-labelled mammalian ICE/CED-3 family members with immobilized RAIDD *in vitro*, and found that RAIDD specifically associated with ICH-1 but not with the other mammalian ICE-like proteases tested (Fig. 2*a*). To see whether this binding was mediated by an NTD–prodomain interaction, we used deletion mutants of ICH-1 and RAIDD (Fig. 2*b*): ICH-1 bound a truncated form of RAIDD containing only the NTD, but not a form containing just the death domain (DD); conversely, ICH-1 without the prodomain did not bind RAIDD whereas the prodomain alone did. These results were confirmed *in vivo* by immunoprecipitating transfected 293 cell lysates for RAIDD (Flag-epitope tagged) and detecting associated molecules by immunoblotting (Fig. 2*c*). To see whether an analogous interaction occurred with CED-3, 293 cells were cotransfected with expression constructs encoding CED-3 and RAIDD or a truncated form of RAIDD lacking the NTD. We found that RAIDD, but not its deleted counterpart, associated with CED-3 (Fig. 2*d*). Together, these results suggest a model in which the NTD by a homophilic mechanism selectively associates with ICE/CED-3 family members by binding to the prodomain.

We further characterized the NTD–prodomain interaction by assaying the binding of wild-type molecules to the corresponding ^{35}S-labelled point mutants within the prodomain of ICH-1 and CED-3 or the NTD of RAIDD (Fig. 3). Mutations were introduced in residues that were highly conserved in all three molecules. More important, however, were alterations in residues

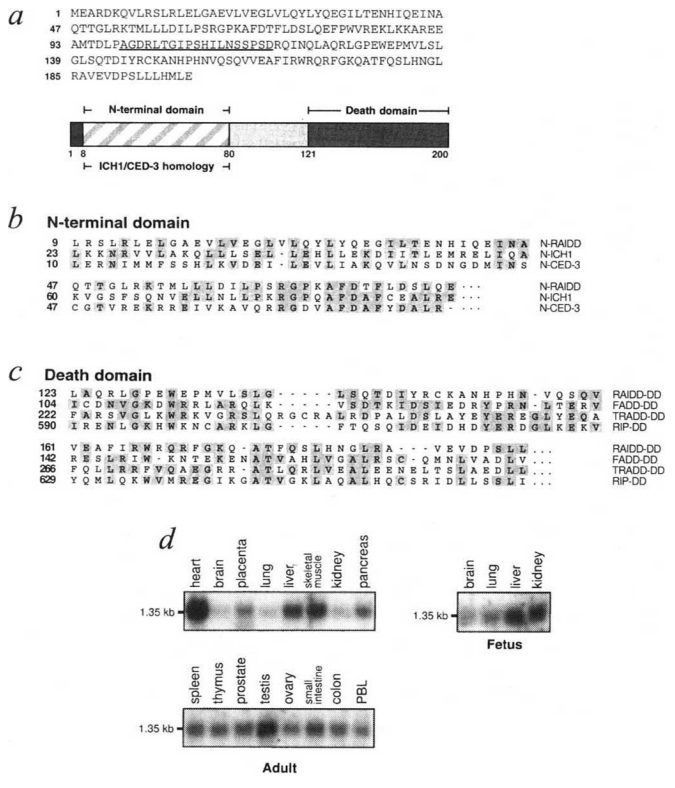

FIG. 1 Sequence characterization and tissue distribution. *a*, Deduced amino-acid sequence of RAIDD. The sequence is underlined of a synthetic peptide (Chiron) used to generate RAIDD antiserum. RAIDD encodes both an N-terminal domain and a C-terminal death domain. *b*, The N-terminal NTD of RAIDD (amino acids 1–80) shares statistically significant homology ($P < 0.001$) with the prodomains of the human cysteine protease ICH-1 (amino acids 1–91) and the *C. elegans* death protease CED-3 (amino acids 1–77). Shading indicates identical residues. *c*, The C-terminal DD of RAIDD (amino acids 123–200) shares sequence similarity with the DD-containing regions of FADD, TRADD and RIP. *d*, Northern blot analysis reveals that RAIDD is expressed in a variety of adult and fetal tissues. PBL, peripheral blood lymphocytes.

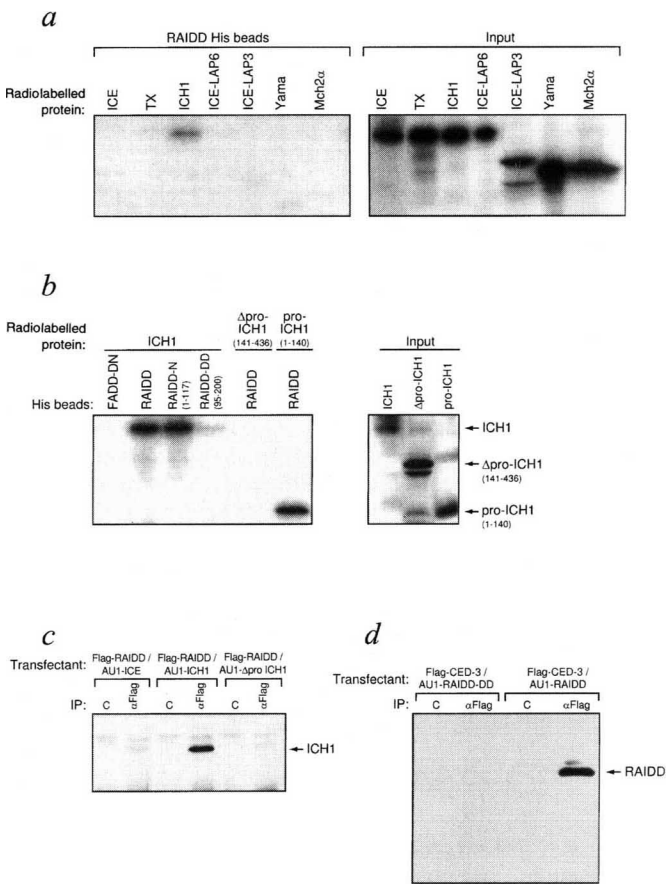

FIG. 2 RAIDD binds ICH-1 and CED-3 *in vitro* and *in vivo*. *a*, Interaction of *in vitro* translated ^{35}S-labelled members of the ICE/CED-3 family with His-tagged RAIDD. Approximate equivalence of input radiolabelled protein is shown on the right. *b*, ICH-1 prodomain binds to the N-terminal domain of RAIDD. ^{35}S-labelled ICH-1 or truncated version that include ICH-1 without the prodomain (pro-ICH-1) or the prodomain alone (pro-ICH-1) were tested for binding to His-tagged RAIDD or its deleted versions containing the N-terminal domain (RAIDD-N) or the death domain (RAIDD-DD). The corresponding DD-containing region of FADD (FADD-DD) served as a control for nonspecific binding. Approximate equivalence of total input radiolabelled protein is shown on the right. *c*, *d*, *In vivo* association of RAIDD with ICH-1 and CED-3. 293 cells were transfected with the indicated combination of expression constructs encoding Flag-RAIDD, AU1–ICH-1, AU1–pro-ICH-1 (amino acids 141–436) or AU1–ICE as a control (*c*). Flag-CED-3 was co-transfected with either the death domain of RAIDD (AU1-tagged, amino acids 123–200) or the full-length molecule (AU1–RAIDD) (*d*). Cleared cell lysates were immunoprecipitated using the indicated antibody (denoted by prefix α) and analysed by immunoblotting with anti-AU1 mAb (c) or anti-RAIDD antipeptide antibody (*d*). IP, immunoprecipitation; C, control antibody.

Leu 27 and Gly 65 in the prodomain of CED-3, because these correspond to inactivating mutations of the *ced*-3 gene in *C. elegans* designated 1,040 and 718 (refs 7, 8). Residues corresponding to Leu 27 and Gly 65 in CED-3 were also mutated in RAIDD and ICH-1: in all Leu-27 or Gly-65 mutants binding was prevented, highlighting the importance of these residues in the prodomain–NTD interaction (Fig. 3). Mutation of conserved hydrophobic residues in the ICH-1 prodomain, including residues Phe 82, Phe 85 and Leu 89 (mt7, mt5 and mt3, where mt means mutation), abolished binding to the NTD of RAIDD. Surprisingly, it took the mutation of both conserved negatively charged residues (Asp 83 and Glu 87; mt8) to eliminate binding (Fig. 3).

Having established the nature of the interactions of the NTD of RAIDD, we asked which death-domain-containing molecules were engaged by the death domain of RAIDD. We first examined all five known mammalian DD-containing proteins implicated in apoptosis[9]. As RAIDD did not bind *in vitro* to either of the two DD-containing receptors (Fas or TNFR-1) (data not shown), we investigated whether it could bind to the DD-containing-receptor-associated molecules FADD, TRADD or RIP. As shown in Fig. 4*a*, RAIDD specifically bound RIP but not FADD or TRADD *in vivo*. But in the presence of RIP, RAIDD was able to complex with TRADD (Fig. 4*a*). As RIP is a component of the TNFR-1 signalling complex[4], it might recruit RAIDD to the complex; RAIDD, in turn, could recruit ICH-1 and so form a direct link to the effector ICE/CED-3-like death proteases. To test this idea, we transiently transfected 293 cells with expression vectors encoding TNFR-1, DD-containing adaptor molecules (TRADD, RIP, RAIDD, FADD), ICH-1, and ICE as a control (Fig. 4*b*, *c*). As anticipated, TNFR-1 complexed with RAIDD in the presence of TRADD and RIP (Fig. 4*b*), and through RAIDD, ICH-1 was recruited to the signalling complex (Fig. 4*c*). We next tested whether RAIDD, besides engaging the death pathway, could also activate NF-κB, because its upstream partner RIP can participate in both pathways[4]. Transfected RAIDD did not activate an NF-κB reporter construct (data not shown), consistent with a primary role in apoptosis. Our results indicate that RAIDD can function as an adaptor molecule in recruiting the death protease ICH-1 to the TNFR-1 signalling complex.

To address the function of RAIDD in apoptosis, MCF-7 cell lines were transiently transfected with an RAIDD expression construct. These cells underwent apoptosis, which was inhibited by the ICE-peptide inhibitor z-VAD-fmk, a poxvirus-encoded serpin known to inhibit apoptosis, CrmA, and by catalytically inactive ICH-1, which was presumably behaving in a dominant-negative manner by competing out endogenous ICH-1 (Fig. 5). However, mutant ICH-1 or various putative dominant-negative versions of RAIDD were unable to block TNFR-1-induced cell death (data not shown), presumably because the alternative TRADD–FADD–FLICE death pathway was unimpeded.

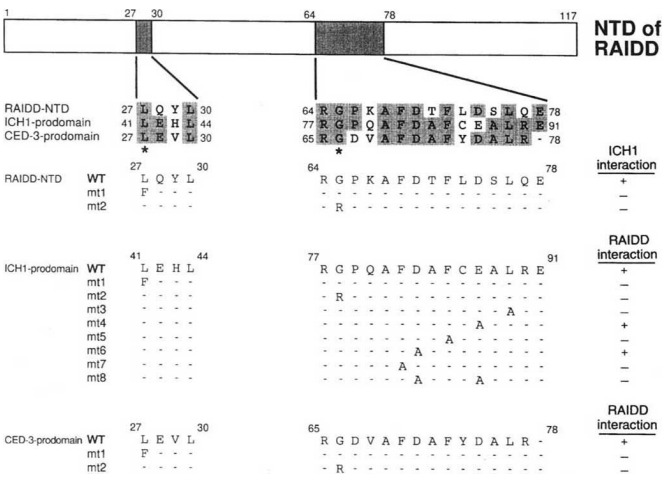

FIG. 3 Mutational analysis of the N-terminal domain in RAIDD and ICH-1. *In vitro* translated ^{35}S-labelled test proteins were incubated with either His-tagged RAIDD immobilized onto Ni^{2+} beads or ICH-1 proteins bound to protein-G–Sepharose. Alignment shows the regions of sequence similarity that surround the two known inactivating mutations in the prodomain of CED-3 (asterisked designated 1,040 and 718). Amino acids within each segment are numbered. Point mutations are shown as altered amino-acid residues aligned with the corresponding wild-type (WT) amino acid. A plus sign indicates significant binding; a minus sign indicates that binding was no different from background.

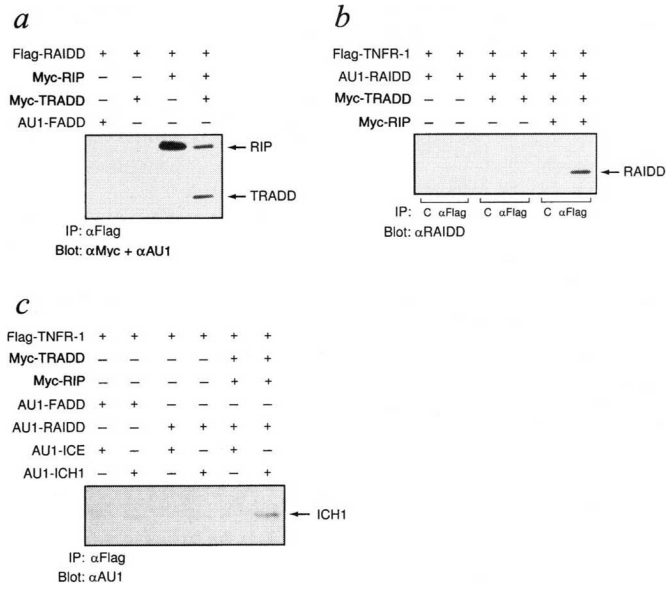

FIG. 4 On overexpression, RAIDD and ICH-1 are recruited to the TNFR1 signalling complex. *a*–*c*, 293 cells were transfected with the indicated combination of expression vectors. Detergent extracts of cells immunoprecipitated with either control mouse IgG or anti-Flag mAb. Co-precipitating proteins were analysed by immunoblotting with anti-epitope tag antibody (anti-Myc and anti-AU1 in *a*; anti-AU1 in *c*; or RAIDD antipeptide antibody in *b*).

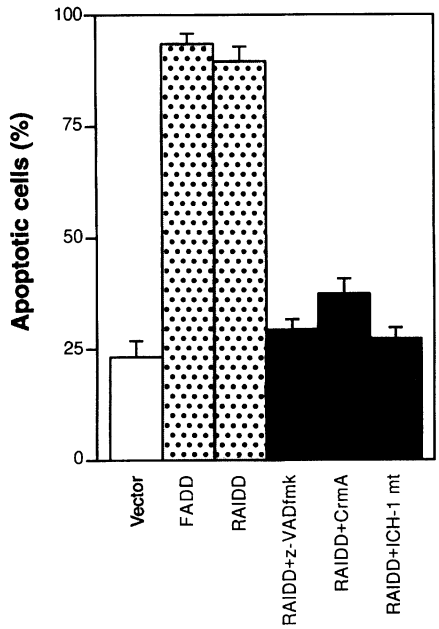

FIG. 5 RAIDD-induced apoptosis. Overexpression of RAIDD induces apoptosis that is inhibitable by CrmA, the broad-range ICE-family inhibitor z-VAD-fmk, and a catalytically inactive version of ICH-1 (Cys 302 → Ala). Data (mean ± s.e.m.) shown are the percentage of apoptotic cells among the total number of cells counted.

It is unclear why two seemingly redundant pathways should be deployed by a single receptor, but they may be used specifically by different cells or tissues. Our results have shown how prodomain interactions can impart binding specificity, a prerequisite for the assembly of a functioning death machine. □

Methods

cDNA cloning. Sequence corresponding to the prodomain of ICH-1 was used to screen the NCBI GenBank EST database using established methods. Several overlapping clones were identified as having statistically significant homology ($P < 0.001$) to the prodomain of ICH-1. One such clone, IMAGE Consortium CloneID 109053 (ref. 10), was characterized further and subjected to both automated and manual DNA sequencing. Additionally, a human K562 cell line cDNA library (from J. Lowe) was screened with a ^{32}P-labelled *PacI/Eco*R1 restriction fragment of the EST clone[11]. Hybridizing clones were characterized by automated sequencing. Sequence assembly, comparison and alignment were performed using DNASTAR software.

Northern blot analysis. Adult and fetal human multiple-tissue northern blots (Clontech) were hybridized according to the manufacturer's instructions with the same ^{32}P-labelled probe that was used for library screening.

Expression vectors. Mammalian cell expression vectors encoding AU1-FADD, Flag-TNFR1, Myc-TRADD and Myc-RIP have been described[4,12]. AU1-RAIDD or Flag-RAIDD was generated by polymerase chain reaction (PCR) using custom-made oligonucleotide primers encoding the AU1 or Flag epitope. Amplified fragments were cloned into the mammalian expression vector pcDNA3 (Invitrogen). In-frame deletion mutants were generated by PCR with or without an N-terminal AU1 epitope and then subcloned into pcDNA3. Point mutants were created by site-directed mutagenesis using a two-step PCR method[13] and confirmed by sequencing. A catalytically inactive ICH-1 was created by mutating the active-site Cys 302 to alanine.

***In vitro* binding assay.** Constructs encoding His-tagged proteins were prepared in the prokaryotic expression vector pET23b (Novagen). Tagged proteins were expressed, purified and immobilized onto Ni^{2+} beads according to standard methodology. GST–Fas and –TNFR-1 fusion proteins were prepared as before[12]. ^{35}S-labelled proteins were obtained by *in vitro* transcription/translation using a TNT T7-coupled reticulocyte lysate system (Promega). After translation, equivalent amounts of ^{35}S-labelled proteins were incubated with His-tagged proteins or GST fusion proteins immobilized onto Ni^{2+} beads or glutathione beads, respectively, as described[12,14]. Beads were washed, boiled in SDS-sample buffer, and eluted proteins were resolved by SDS–PAGE and autoradiographed. Alternatively, ICH-1 protein was produced in human 293 embryonic kidney cells transfected with the AU1-ICH1 expression construct.

Transfection, coimmunoprecipitation and western analysis. 293 cells were transiently transfected with the indicated plasmids, lysed in 1 ml buffer (50 mM Tris, pH 7.6, 150 mM NaCl, 0.1% NP-40) and incubated either with mouse control IgG or anti-Flag mAb. Immune complexes were precipitated by the addition of protein-G–Sepharose (Sigma). After extensive washing, the Sepharose beads were boiled in sample buffer and the eluted proteins processed as before[15].

Apoptosis assay. MCF-7 human breast carcinoma cells, CrmA-expressing stable cell lines[16], or 293-EBNA cells were transiently transfected with 0.25 μg of the reporter plasmid pCMV–β-gal plus 1.5 μg of test plasmid encoding either FADD or RAIDD. The broad spectrum ICE-family inhibitor z-VAD-fmk (Enzyme Systems Products) was added to the cells at 20 μM, 5 h after transfection. 48 h later, apoptosis assay was as described[12].

Received 12 September; accepted 18 November 1996.

1. Fraser, A. & Evan, G. *Cell* **85,** 781–784 (1996).
2. Henkart, P. *Immunity* **4,** 195–201 (1996).
3. Stanger, B. Z., Leder, P., Lee, T. H., Kim, E. & Seed, B. *Cell* **81,** 513–523 (1995).
4. Hsu, H., Huang, J., Shu, H.-B., Baichwal, V. & Goeddel, D. V. *Immunity* **4,** 387–396 (1996).
5. Wang, L., Miura, M., Bergeron, L., Zhu, H. & Yuan, J. *Cell* **78,** 739–750 (1994).
6. Yuan, J., Shaham, S., Ledoux, S., Ellis, H. M. & Horvitz, H. R. *Cell* **75,** 641–652 (1993).
7. Ellis, H. M. & Horvitz, H. R. *Cell* **44,** 817–829 (1986).
8. Shaham, S. & Horvitz, H. R. *Genes Dev.* **10,** 578–591 (1996).
9. Cleveland, J. L. & Ihle, J. N. *Cell* **81,** 479–482 (1995).
10. Lennon, G., Auffray, C., Polymeropoulos, M. & Soares, M. B. *Genomics* **33,** 151–152 (1996).
11. Sambrook, J., Fritsch, E. F. & Maniatis, T. *Molecular Cloning: A Laboratory Manual* 2nd edn (Cold Spring Harbor Laboratory Press, New York, 1989).
12. Chinnaiyan, A. M., O'Rourke, K., Tewari, M. & Dixit, V. M. *Cell* **81,** 505–512 (1995).
13. Higuchi, R., Krummel, B. & Saiki, R. K. *Nucleic Acids Res.* **16,** 7351–7367 (1988).
14. Muzio, M. *et al. Cell* **85,** 817–827 (1996).
15. O'Rourke, K. M., Laherty, C. D. & Dixit, V. M. *J. Biol. Chem.* **267,** 24921–24924 (1992).
16. Tewari, M. & Dixit, V. M. *J. Biol. Chem.* **270,** 3255–3260 (1995).

ACKNOWLEDGEMENTS. We are especially grateful to H. R. Horvitz for *ced*-3 cDNA and D. V. Goeddel for RIP and TRADD expression constructs; we thank K. O'Rourke, A. M. Chinnaiyan and C. Vincenz for discussion and for material assistance, and I. Jones for help in preparing the figures.

CORRESPONDENCE and requests for materials should be addressed to V.M.D. (e-mail: vmdixit@umich.edu). The nucleotide sequence reported here has been submitted to the GenBank/EMBL Data Bank (accession number U79115).

Brain acetylhydrolase that inactivates platelet-activating factor is a G-protein-like trimer

Yew S. Ho, Lora Swenson*, Urszula Derewenda, Laurence Serre*†, Yunyi Wei, Zbyszek Dauter‡, Mitsuharu Hattori§, Tomoya Adachi§, Junken Aoki§, Hiroyuki Arai§, Keizo Inoue§ & Zygmunt S. Derewenda

Department of Molecular Physiology and Biological Physics, University of Virginia Health Sciences Center, PO Box 10011, 1300 Jefferson Park Avenue, Charlottesville, Virginia 22906-0011, USA
* Department of Biochemistry, University of Alberta, Edmonton, Alberta T6G 2H7, Canada
‡ EMBL Outstation, 22603 Hamburg, Germany
§ Department of Health Chemistry, Faculty of Pharmaceutical Sciences, The University of Tokyo, Hongo 7-3-1, Bunkyo-ku, Tokyo 113, Japan

THE platelet-activating factor PAF (1-*O*-alkyl-2-acetyl-*sn*-glycero-3-phosphocholine) is a potent lipid first messenger active in general cell activation, fertilization, inflammatory and allergic reactions, asthma, HIV pathogenesis, carcinogenesis, and apoptosis[1–5]. There is substantial evidence that PAF is involved in intracellular signalling, but the pathways are poorly understood. Inactivation of PAF is carried out by specific intra- and extracellular acetylhydrolases[6] (PAF-AHs), a subfamily of phospholipases A2 that remove the *sn*-2 acetyl group. Mammalian brain contains at least three intracellular isoforms, of which PAF-AH(Ib) is the best characterized[7–9]. This isoform contains a heterodimer of two homologous catalytic subunits α_1 and α_2, each of relative molecular mass 26K, and a non-catalytic 45K β-subunit, a homologue of the β-subunit of trimeric G proteins. We now report the crystal structure of the bovine α_1 subunit of PAF-AH(Ib) at 1.7 Å resolution in complex with a reaction product, acetate. The tertiary fold of this protein is closely reminiscent of that found in p21^{ras} and other GTPases. The active site is made up of a trypsin-like triad of Ser 47, His 195 and Asp 192. Thus, the intact PAF-AH(Ib) molecule is an unusual G-protein-like (α_1/α_2)β trimer.

Mammalian brain contains significant levels of PAF, which acts as a synapse messenger and transcription inducer of the early-response genes c-*fos* and c-*jun*[10]. It accumulates rapidly in neural tissue during seizures or ischaemia[11] and the resulting brain damage can be reduced by PAF antagonists[12]. PAF is also being implicated as a messenger in long-term potentiation, a cellular model of memory formation[13]. The β-subunit of the PAF-AH(Ib) complex is a product of the gene that is responsible for the onset of type-1 lissencephaly, a developmental brain disorder caused by impaired neuronal migration, in which no cortex is formed[14]. This suggests a potential role for PAF in early brain development and neuronal migration.

The two catalytic α-subunits of PAF-AH(Ib) (this new notation is consistent with that accepted for the structurally related G-protein subunits) share extensive amino-acid sequence identity—63% in the bovine form[9]—but the consensus sequence they share is unique among proteins. When these subunits are purified or overexpressed individually in *Escherichia coli*, they form catalytically competent homodimers. *In vivo*, however, α_1 is preferentially labelled by [1,3-^{3}H]diisopropyl fluorophosphate in the heterodimer, suggesting functional asymmetry[9].

The PAH-AH(Ib) α_1 subunit is a single polypeptide chain of 231 residues[7]. The molecule contains a single α/β domain with a central, parallel, 6-stranded β-sheet. This fold is very like that found in GTPases (Fig. 1*a*, 2). The insertions and deletions in the

† Present address: Institute de Biologie Structurale (IBS), Avenue des Martyrs, 38042 Grenoble Cedex, France.